Yes

THE NATURAL RADIATION ENVIRONMENT

J. Warren Keller
Chief, Space Vehicle Environmental Factors
Office of Advanced Research and Technology
NASA Headquarters
Washington, D. C.

Paper Presented at Institute of Environmental Sciences Symposium
February 26, 1964
University of Michigan
Ann Arbor, Michigan

RADIATION ENVIRONMENT IN SPACE

Introduction

In the last few years, data have been gathered which indicate that one of the major environmental factors which must be considered for any space vehicle is that of radiation. The radiation environment has been found to be an important consideration not only for those vehicles which carry a reactor on board for propulsion or power but for all vehicles since they will be exposed to the indigenous radiations in space (i.e. galactic cosmic rays, solar protons, geomagnetically trapped radiation).

On board reactor sources present, in general, a fixed source of radiation with the intensity of the leakage radiation being dependent upon the time profile of the power but with the spectral, angular, and spatial distributions remaining more or less constant and determined to a large degree by the geometry of the particular vehicle. On the other hand, the various components of the indigenous radiations are known to vary greatly in spectral, angular, and spatial distributions as well as in composition depending upon position and time.

The purpose of this paper is to convey in simple terms the current picture of the important components (for space vehicle design) of the indigenous radiation fields in space, including galactic cosmic radiation, solar cosmic radiation (solar protons), and the geomagnetically trapped radiation both from natural origin and from the July 1962 high altitude nuclear detonation.

Galactic Cosmic Radiation

Galactic cosmic radiation presents a more or less constant (except for solar modulation) environmental factor to which any space vehicle will be subjected. From high altitude balloon and rocket measurements over the last decade or so the particle composition of the primary radiation has been quite well determined. Also, using the earth's magnetic field as a momentum selector, the energy spectrum has been determined.

The composition of the primary cosmic radiation which consists largely of energetic nuclei which have been stripped of their electrons has been found to be as follows; $\sim$85% hydrogen, $\sim$12% helium, $\sim$1% in the carbon-nitrogen-oxygen group, $\sim$ 0.25% in the lithium-beryllium-boron group, $\sim$ 0.25% neon and heavier. High energy electrons constitute the remainder of the total flux.

The energies of the primary particles extend from below 10^8 electron volts to as high as about 10^{19} electron volts. All the charged components have been observed to exhibit energy spectra of the same form in the high-energy region ($E > 3$ Bev), which may be represented for a given Z by

$$N(>E) = \frac{C}{(1+E)^{\gamma}}$$

where $N(> E)$ is the flux in particles/cm^2-sec-ster with energy $> E$, E is the energy per nucleon in Bev, γ is a constant which is independent of Z (atomic number) and C is a constant. In the energy region between 300 Mev and 3 Bev the various components seem to have similar spectral forms when expressed in terms of magnetic rigidity while at energies below 300 Mev the spectral form is questionable.

The angular distribution of the galactic cosmic rays has been found to be isotropic. With the total flux being about 2 cm^{-2}-sec^{-1} at solar maximum and about 4 cm^{-2}-sec^{-1} at solar minimum. The galactic cosmic ray intensity has been shown to undergo modulations which may be correlated with solar activity. One such modulation is that connected with 11-year solar cycle. The correlation, here, with solar activity is a negative one - that is, the cosmic ray intensity decreases as solar activity increases. As indicated, above, a variation in flux of about a factor of 2 is observed over the solar cycle. In addition to the 11-year cycle modulation the galactic cosmic ray intensity is subject to rather sudden decreases. These short term changes are called Forbush decreases and may be correlated with large magnetic storms. These decreases which usually occur at times of high solar activity result in a 25% to 30% decrease in the already reduced intensity. In both types of modulations it is principally the lower energy particles which are affected.

Since the primary cosmic particles apparently originate for the most part from sources external to our solar system and are observed to be isotropic it is obvious that they should be expected to present essentially a constant environment for a space vehicle regardless of its location. Fortunately, however, the intensity of the radiation is so small that it does not deserve any great concern from the point of view of radiation damage to components or materials and perhaps only limited concern as far as man is concerned at least for short missions.

The energy flux at the vicinity of the earth over 2π steradians is $\sim 7 \times 10^{-3}$ ergs-cm^{-2}-sec^{-1} with the energy density being ~ 0.6 ev/cm^3, about that of starlight.

It is indeed fortunate that the flux of these particles is not large since their very high energies make them very difficult to shield against.

Solar Cosmic Radiation

Another type of radiation environment which one would apparently encounter throughout the solar system is the solar cosmic radiation or "solar protons." These names are used to describe the large fluxes of energetic particles which are observed to reach the vicinity of the earth following a portion of the intense solar flares which occur on the surface of the sun.

While the galactic cosmic radiation has been known and studied for many years the solar cosmic radiation was discovered less than 20 years ago and has been studied in detail only for the last 7 years. Such studies have utilized ground level neutron and radio absorption measurements as well as measurements made on high-altitude balloons, satellites and space probes.

The particles observed following a solar outburst are predominantly protons whose energies extend to as high as several Bev in some cases - hence, the name "solar protons." In each event, however, particles heavier than protons appear to be present. The relative number of heavier particles (mostly alpha particles) varies greatly from event to event.

Figure 1 shows the time of occurrence and the relative magnitude of 29 solar proton events during the years 1956 through 1961 which exhibited an integrated intensity of greater than 10^6 protons/cm^2 for energies greater than 30 Mev. The figure is based on data given in Reference 1. There are several observations which may be made from this figure. The sporadic nature of the time interval between events is notable with the "bunching" of events being the result of several outbursts originating in the same active region on the sun. As a matter of fact, the events shown represent only 16 active regions with 90 percent of all the solar cosmic rays during the six year period having originated in only four of those regions. Also of interest is the fact that none of the largest events occurred during the years of solar maximum (1957-58) but, instead, occurred on either side of the maximum particularly on the decreasing side. Notable is the relatively long period between the occurrences of active centers which have produced such large events.

Since the length of time over which detailed observations have been made is small and the statistics are few, it cannot be said with any degree of certainty that the largest events which are possible have been observed. Also, it is obviously improper to correlate size or frequency of events with sun spot cycles when one considers that detailed observations have been made during but one such cycle.

Figure 2 (taken from Reference 1) shows the yearly integrated intensities of solar particles above 100 Mev as well as 30 Mev compared with the total yearly integrated intensitites of galactic particles. It is obvious that the large events constitute the major part of the flux.

Figure 1. Frequency and Intensity of Solar Cosmic Radiation Events

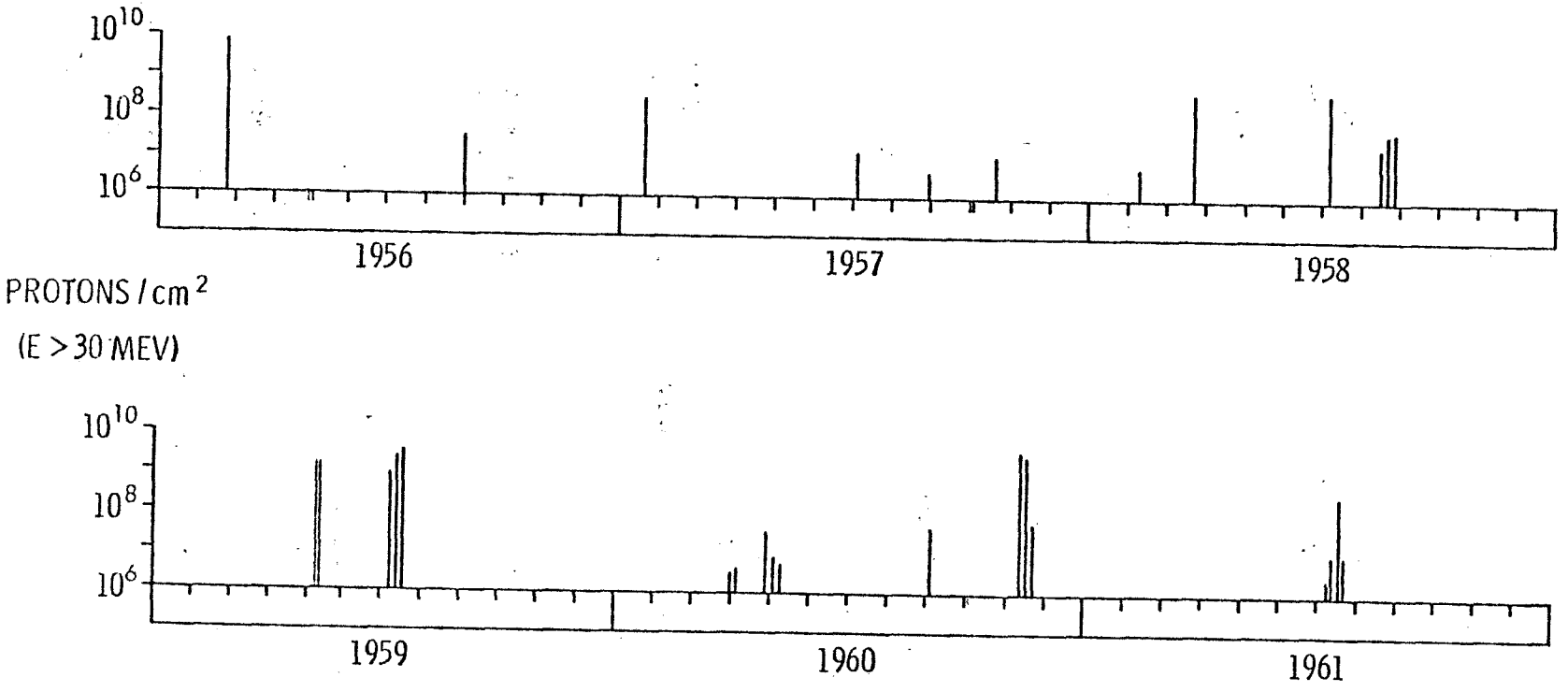

NASA RV63 - 1378

Figure 2.

YEARLY INTEGRATED INTENSITIES OF SOLAR COSMIC RAYS WITH ENERGIES ABOVE 30 AND 100 MEV AND OF GALACTIC COSMIC RAYS

YEAR	NUMBER OF EVENTS	SOLAR COSMIC RAYS INTEGRATED INTENSITY (PARTICLES / CM^2)		GALACTIC COSMIC RAYS INTEGRATED INTENSITY (PARTICLES / CM^2)
		> 30 MEV	> 100 MEV	
1956	2	8×10^9	8×10^8	1×10^8
1957	4 OR 5	4×10^8	1.5×10^7	7×10^7
1958	6	1×10^9	1.4×10^7	6×10^7
1959	4	7×10^9	5.2×10^8	6×10^7
1960	8	5×10^9	4.1×10^8	8×10^7
1961	5	27×10^8	3.3×10^7	1×10^8
TOTAL	30	2.1×10^{10}	1.8×10^9	4.7×10^8

NASA RV63 - 1368

Solar proton events are characterized, in general, by a relatively rapid rise to maximum intensity followed by a slower decay. However, the time constants associated with these characteristics along with the time from the flare occurrence to the arrival of particles vary from event to event and with energy. The delay in particle arrival as well as the rise time may vary from a few minutes for high energy particles in one event to many hours for low energy particles in another. The decay in intensity may be represented (Ref. 2) by an expression of the form

$$I(E) = I_{max}(E)\, e^{-t/t_D}$$

where I(E) is the intensity at time, t after $I_{max}(E)$ of particles having energies greater than E, and t_D is the "decay time" which is a function of energy, E, and varies from event to event. The decay time may range from 3-4 hours for high energy particles in one event to 2-3 days for low energy particles in another.

Since the decay time, the delay time for particle arrival, and the rise time are functions of energy it is obvious that the energy spectrum for a given event must change with time. Indeed, the spectrum does vary, becoming softer and softer with time throughout an event.

A spectral and intensity variation for a "typical" large solar flare event has been proposed by Dr. D. K. Bailey (Ref. 3). This hypothetical solar proton event represents an attempt at correlating continuous radio observations with direct balloon, satellite, and rocket observations. A cross plot of Bailey's flux versus energy curves

(time as a parameter) are shown in Figure 3(a) in the form of integral flux as a function of time with energy as the parameter. The dashed portion of the curves represent extrapolations in time beyond that given by Bailey. Many of the typical characteristics discussed earlier are illustrated by the curves. The totally dashed curve represents a curve derived by Fichtel, Guss, and Ogilvie (Ref. 4) to envelope the highest fluxes greater than 100 Mev which have been experimentally observed for solar proton events to date and is included for comparison with the Bailey "typical" event. The time integrated integral and differential spectra derived from the curves in Figure 3(a) are shown in Figure 3(b).

Many persons not close to the problem appear to be of the opinion that since the solar protons originate at the sun they must arrive from the direction of the sun. The evidence to date indicates that this picture is incorrect since for the most part, the particles arrive isotropically. It appears, however, (Ref. 5) that in some cases the flux is anisotropic for the first 1-2 hours after which it becomes isotropic. In all such cases probably less than 20 percent of the radiation dose arrives during the period of anisotropy.

When one considers the total flux greater than 30 Mev (corresponding to range of 1 gm/cm^2) given in Figure 2 for the period from 1956 through 1961, he must conclude that the radiation effects problem from solar protons for most items internal to the space vehicle other than humans may be quite small since this total flux is just about the level for obtaining significant damage in the most sensitive semiconductor devices

Figure 3. Spectral Characteristics of Bailey's "Typical" Flare

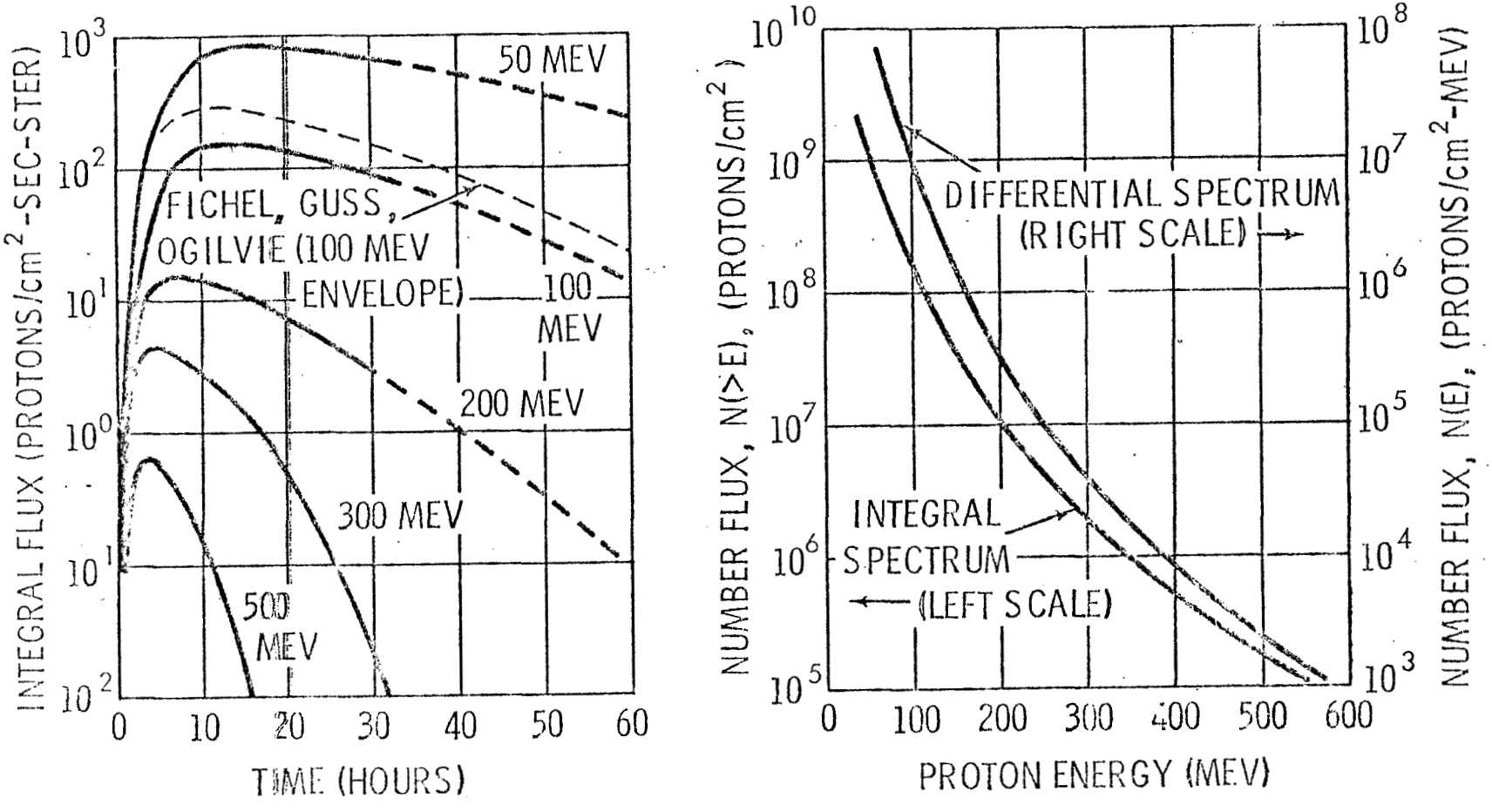

(A) TIME VARIATION OF INTEGRAL FLUX

(B) TIME INTEGRATED SPECTRA

NASA RV63 - 1379

(i.e. solar cells). Unfortunately, insufficient data have been obtained on the energy spectrum at low energies to allow an accurate determination of the effects on such sensitive items external to the vehicle.

Geomagnetically Trapped Radiation

The radiation in space which appears to present by far the most difficult problem from the radiation effects viewpoint and is of the most immediate concern is that which is trapped in the magnetic field of the earth. Included are the protons and electrons which constitute the natural Van Allen belt along with the electrons injected as a result of the July 1962 high-altitude nuclear detonation.

Natural Radiation Belt - The natural geomagnetically trapped radiation was first detected by the instrumentation on the Explorer I. Subsequently, it has been studied by the use of radiation detectors on virtually all the succeeding satellites.

This radiation consists of charged particles (protons and electrons) trapped along the lines of force in the earth's magnetic field. The early picture (Ref. 6) of the trapped radiation was as shown in Figure 4, where the contour lines represent the counting rates obtained with Geiger counters flown in Explorer IV and Pioneers III and IV. The picture was of two belts extending in doughnut fashion around the earth with the inner belt being composed of both protons and electrons and the outer belt predominantly of electrons.

Over the course of time as a result of numerous space experiments, the picture has evolved into the one illustrated in Figure 5 (based on

Figure 4. Early Picture of Natural Radiation Belts

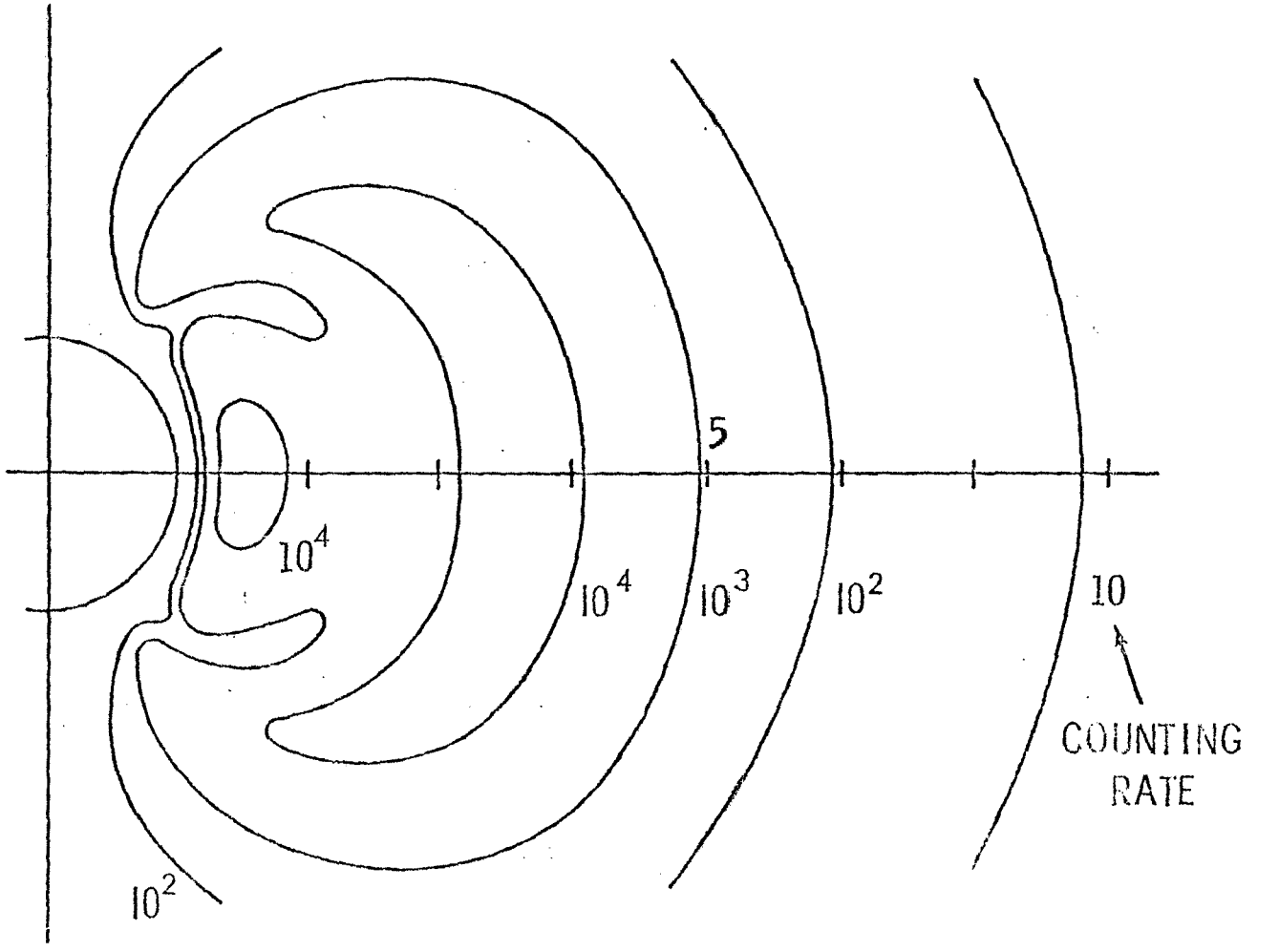

NASA RV63 - 1374

Reference 7). Here, each of the components illustrated extends over both hemispheres and must be rotated about the vertical axis to give the three dimensional picture. The data on the right for protons greater than 30 Mev and electrons greater than 1.6 Mev are seen to correspond with the picture given in Figure 4. However, it is seen that when one considers the data presented on the left for protons between 0.1 Mev and 5 Mev and for electrons greater than 40 Kev, it is no longer proper to speak of two distinct belts having different particle compositions. Indeed, it is apparent that the two belt concept came as a result of the high threshold of the detectors used.

The charged particles which are trapped in the magnetic field spiral along the lines of force with one of the constants of the motion being represented by

$$\frac{\sin^2\theta}{H} = \frac{\sin^2\theta_o}{H_o} = \text{constant}$$

where θ is the angle between the particle velocity and the line of force and H is the field strength with the subscript, o, referring to the equatorial plane. As the particle travels in a spiral about the magnetic field line toward higher latitudes, it travels into a converging field resulting in an increase in H and, hence, an increase in pitch angle, θ. When θ reaches 90 degrees the particle is reflected, again spiraling about the line of force until reaching the corresponding point in the opposite hemisphere where it is again reflected. It is seen that the smaller the pitch angle in the equatorial plane, the deeper into the

Figure 5. Present Picture of Natural Radiation Belts

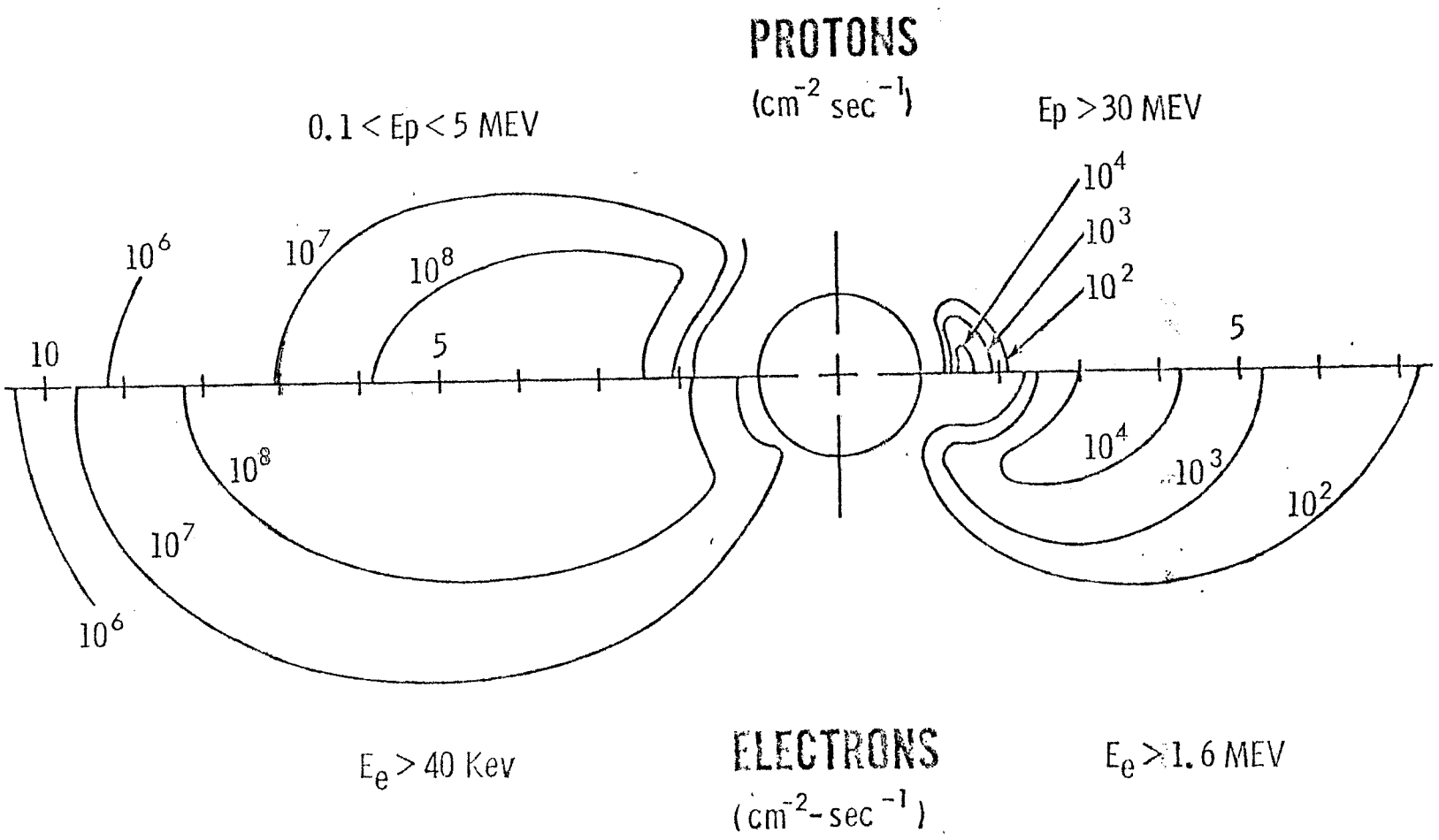

NASA RV63 - 1373

atmosphere will be the point of reflection (mirror point). Consequently, those particles having small pitch angles will be absorbed leaving the radiation at all points peaked in the directions perpendicular to the lines of force with the peaking more pronounced at high latitudes.

Since the earth's magnetic field has a gradient across the lines of force as well as along them, there exists a particle drift in longitude. This drift, to the east for negatively charged particles and to the west for positively charged particles, is caused by the change in the radius of curvature of the particle motion along a single rotation. This being the case, regardless of the point of injection, in time the radiation spreads around the earth.

In carrying out this motion, the particle will remain along lines of force exhibiting field strengths corresponding to those along the original line. Since the earth's magnetic field is not a true dipole, the particles will vary in altitude as they circle the earth and consequently the altitude of the bottom of the radiation belt will be a function of longitude. This variation which is often neglected when determining the radiation to which a vehicle will be subjected is shown in Figure 6 (taken from Reference 8). Here the geographical latitude and longitude for the geomagnetic equator are shown with the altitudes of the belt bottom in the geomagnetic equatorial plane. It is seen that a variation of as much as $\sim$1000Km exists in the altitude of the belt bottom from one longitude to another. This could result in a significant error if not considered. As a result of the expansion of the

Figure 6. Location of Bottom of Natural Radiation Belt

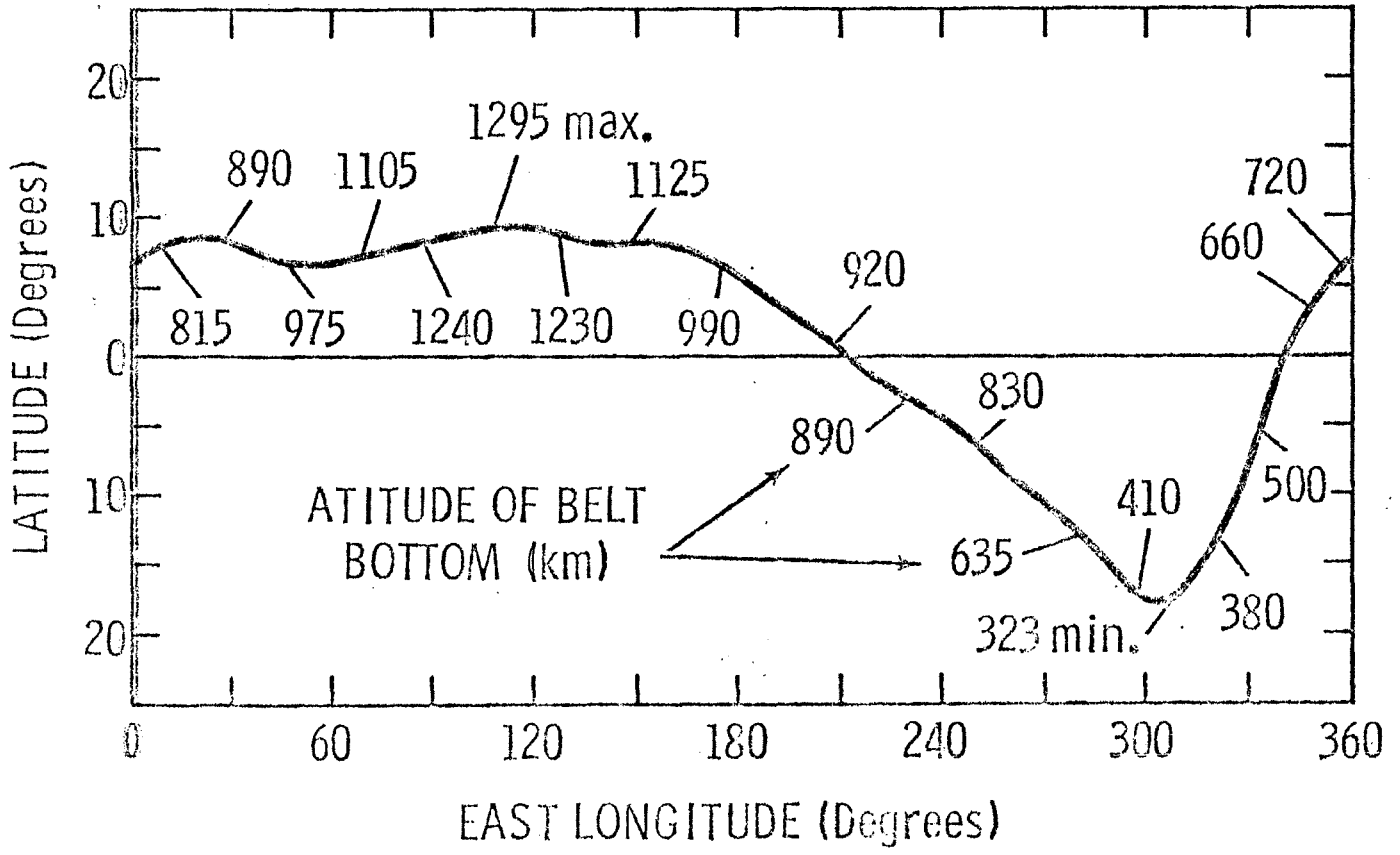

NASA RV63 - 1367

atmosphere from increased heating during solar maximum, the height of the belt bottom also varies with time.

The only practical way which has been developed (Ref. 9) for considering the variations in the earth's field is to represent both the spatial distribution of the radiation and the vehicle trajectory in the "natural" geomagnetic coordinates, B and L, where B is the magnetic field strength and L designates the magnetic shell on which the particle travels as it drifts in longitude. Numerically, L is equal to the distance from the earth's center (in earth radii) to the shell if the field were an ideal dipole.

The two belt concept does persist with a different distinction between the belts than in the original case. The distinctive characteristic of the inner belt is its stability with time whereas the outer belt undergoes orders of magnitude changes in intensity within times of the order of days or even hours. An L value of about 2 seems to form the dividing point between the belts.

The energies of the trapped protons extend to hundreds of Mev. Measurements have been made of the spectra of the penetrating protons in the inner zone. Freden and White (Ref. 10) found the proton spectrum between 75 Mev and 700 Mev at altitudes of ~1000 to 1200 Km and L = 1.4 to be of the form

$$N(E_p)\,dE \approx K E_p^{-1.8}\,dE$$

where K is a constant and E_p the proton energy. This expression has

received wide usage. At lower energies (<100 Mev), the spectrum has been found by Naugle and Kniffen (Ref. 11) to become systematically softer with increasing L. McIlwain and Pizzella (Ref. 12) have since analyzed Explorer IV data to obtain an expression for this variation which fits other measurements reasonably out to L ≈8. The expression is

$$N(E_p)dE = (\text{constant})\, e^{-E_p/E_o}\, dE$$

with

$$E_o = (306 \pm 28)\, L^{-(5.2 \pm 0.2)} \text{ Mev}$$

The shape of the Freden and White spectrum is compared in Figure 7 with the integrated spectrum from the Bailey "typical" flare. It is noted that the trapped protons exhibit a much harder spectrum than those resulting from solar flares, thus, presenting a much more formidable problem where shielding is required.

Very little is known about the energy spectrum of electrons in the region of the inner belt (L <2). Several measurements have been made at low altitudes but the agreement is not good. This situation is not expected to improve soon since the natural radiation is now masked by the presence of the artificial electron belt which will be discussed in the next section.

A goodly number of measurements have been made of the spectrum of the outer belt electrons. However, it is impossible to speak of any one spectral shape as the spectrum because of the large temporal variations

Figure 7. Spectral Shapes of Solar and Trapped Protons

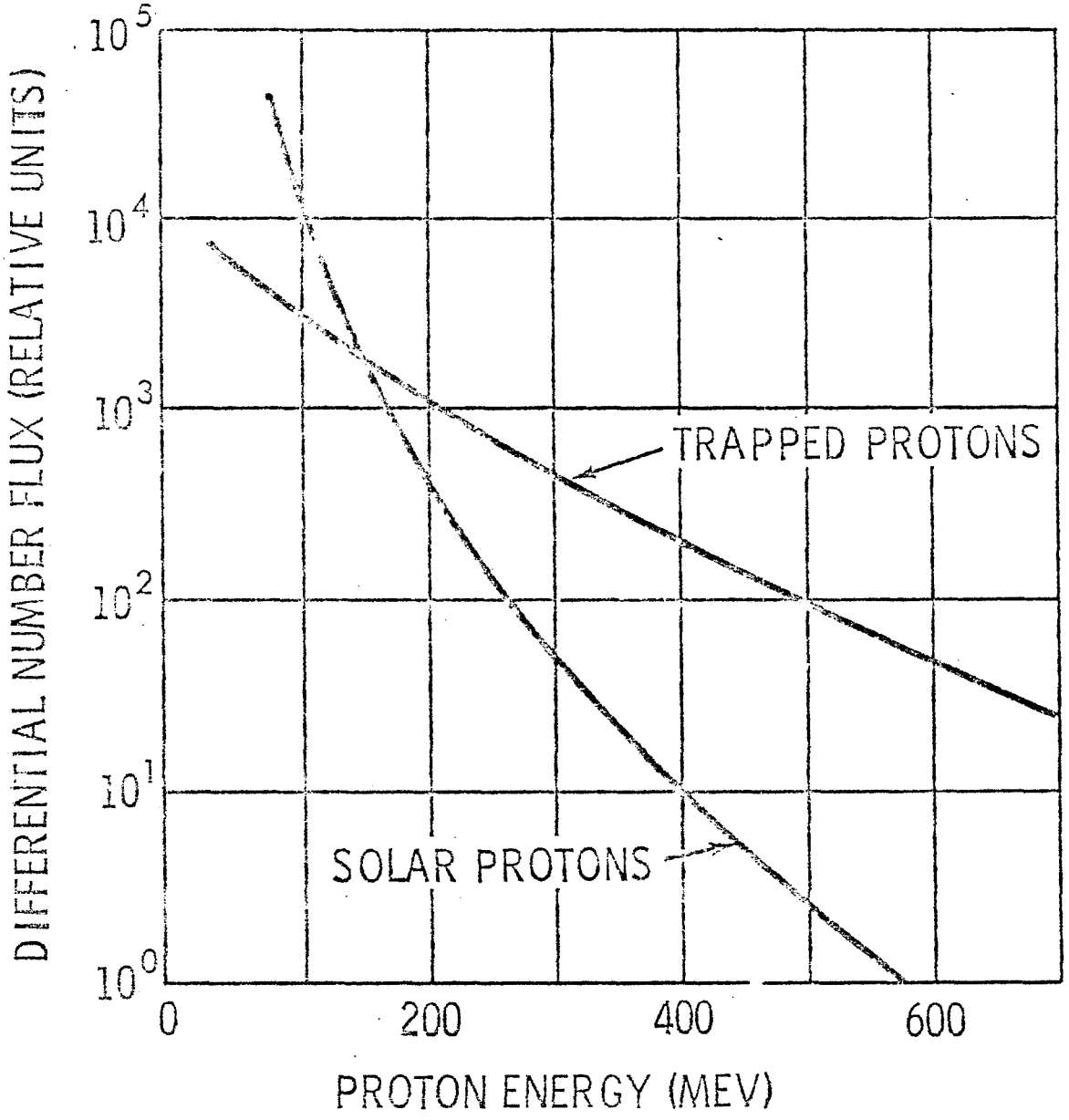

NASA RV63- 1369

which are encountered. One spectral shape obtained by O'Brien et al (Ref. 13) is compared in the next section (Fig. 10) with that of the artificial belt of electrons.

The naturally occurring trapped electrons are, for the most part, low enough in energy so that they are readily stopped with only the resulting bremsstrahlung radiation presenting a radiation hazard internal to the vehicle. The protons, however, exhibit a relatively flat spectrum and can present a problem internal as well as external to a space vehicle. As is the case for solar protons, the low energy spectrum is not well enough known to allow an accurate prediction of the effects on sensitive components such as solar cells external to a vehicle.

Artificial Radiation Belt - On July 9, 1962 a nuclear device was detonated at high altitude over Johnson Island in the Pacific. This explosion (code named Starfish) produced a belt of electrons which, trapped in the same manner as the particles in the natural belt, encircled the earth.

The spatial distribution of these particles at a time about one week after the explosion was according to Hess (Ref. 15) as shown in Figure 8. Here the contours of the artificial belt are shown along with those for the high energy naturally occurring protons for comparison. The peak fluxes are seen to be higher than those for the natural electron belts (See Fig. 5).

It is noted from Figure 8 that the high intensity regions of the artificial belt extended to considerably lower altitudes than do those

Figure 8. Flux Contours for High Energy Trapped Protons and Artificial Electron Belt

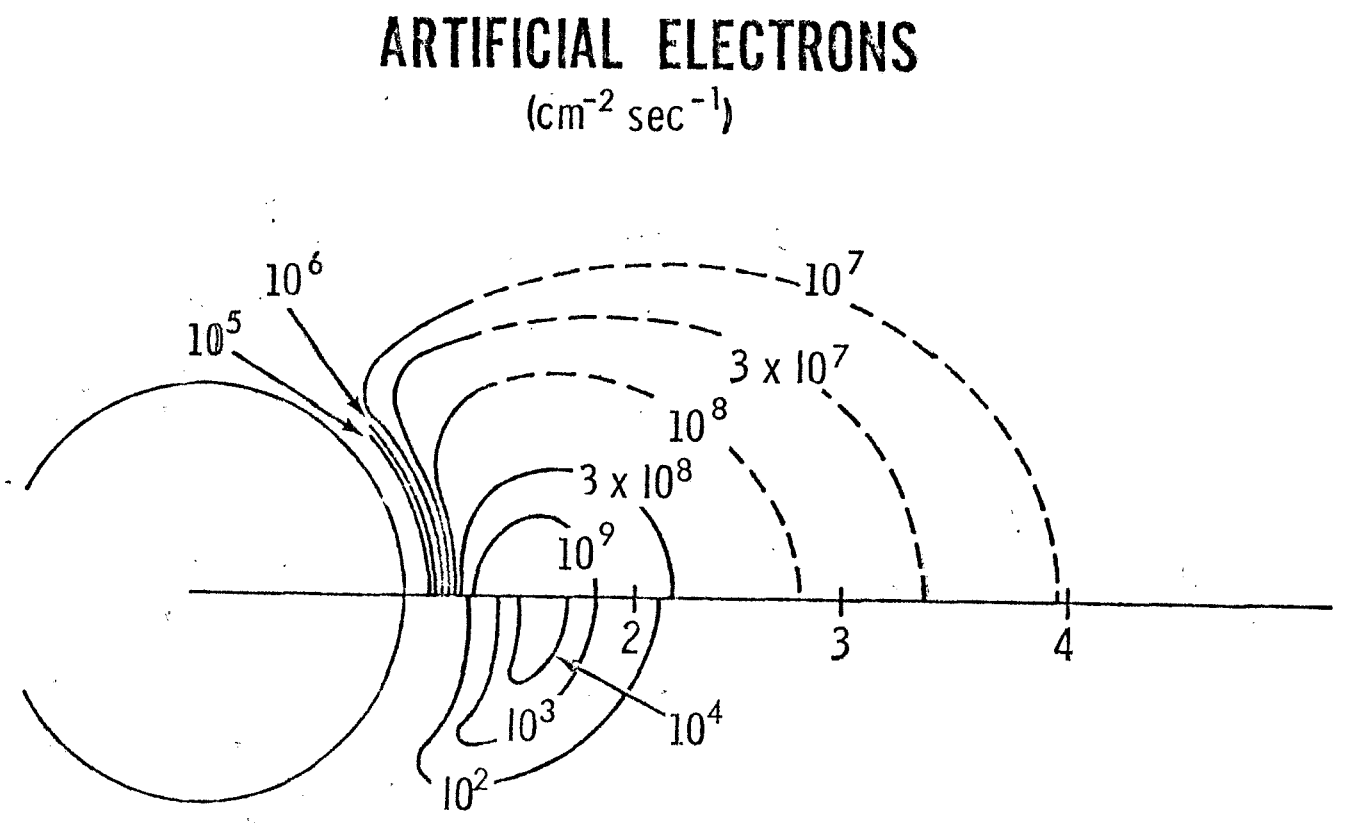

NASA RV63 - 1372

of the natural belts, resulting in a hazard to vehicles which were designed to fly in orbits which were free of significant radiation problems. This hazard is illustrated in Figure 9 which shows the flux contours at an altitude of 400 Km (Ref. 15). Here we see substantial fluxes of particles at an altitude which previous to the Starfish explosion was essentially free of significant radiation hazards. The high fluxes at this altitude are a result of the South Atlantic anomaly in the earth's magnetic field.

The spectrum of the electrons generated by the bomb should be essentially that of electrons from the fission of U^{235}. This spectrum has been determined (Ref. 16) to be given by

$$N(E)\,dE = 3.88\, e^{-0.575E - 0.055E^2}$$

for E between 1 and 7 Mev. Figure 10 is a comparison of this spectrum with that measured in the outer natural electron belt by O'Brien et al (Ref. 13). The relative intensities in the plot have no meaning. It is seen that the electrons in the artificial belt are, on the whole, much more energetic ranging to as high as 6 or 7 Mev and, hence, more penetrating.

The results of calculations, by the author, of the dose due to penetrating electrons and bremsstrahlung behind aluminum shields for an incident fission electron spectrum normalized to one electron/cm^2 incident are shown in Figure 11. It is seen that the penetrating electrons constitute the major portion of the dose for shield thicknesses

Figure 9. Flux Map for Artificial Electron Belt at 400 Km Altitude

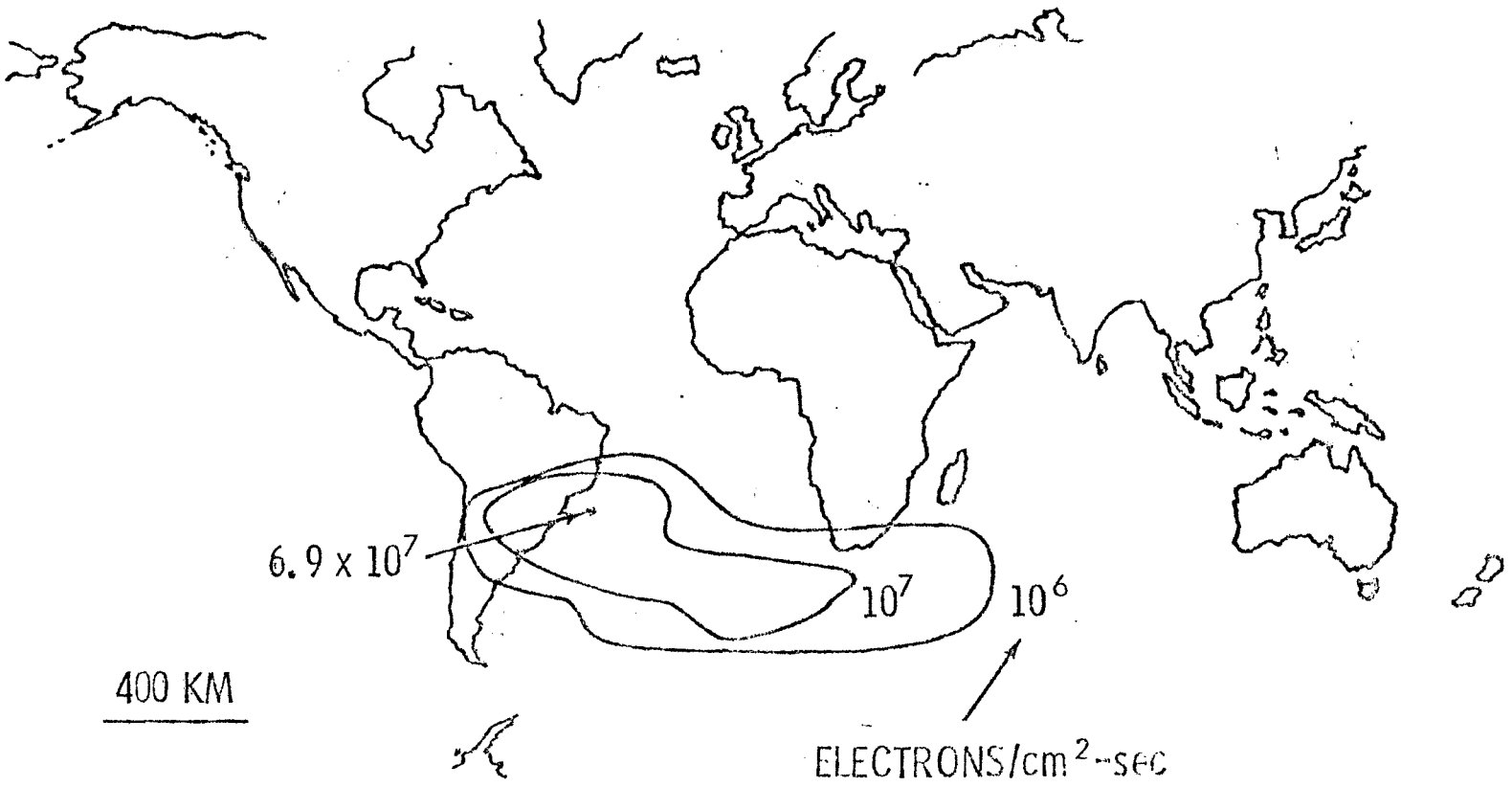

Figure 10. Spectral Shapes of Natural and Artificial Electrons

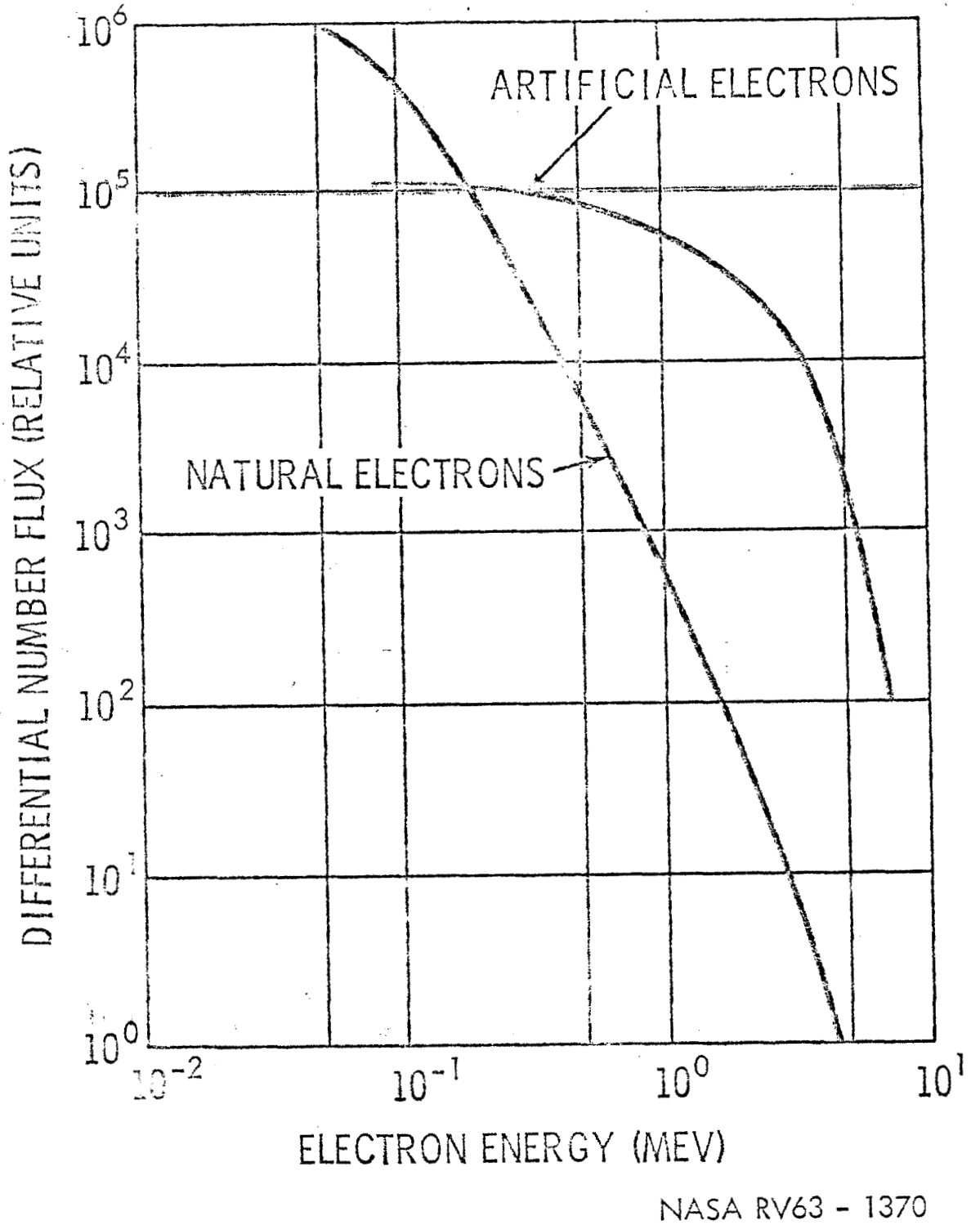

NASA RV63 - 1370

Figure 11. Shielding Effectiveness of Aluminum for Fissions Electron Spectrum

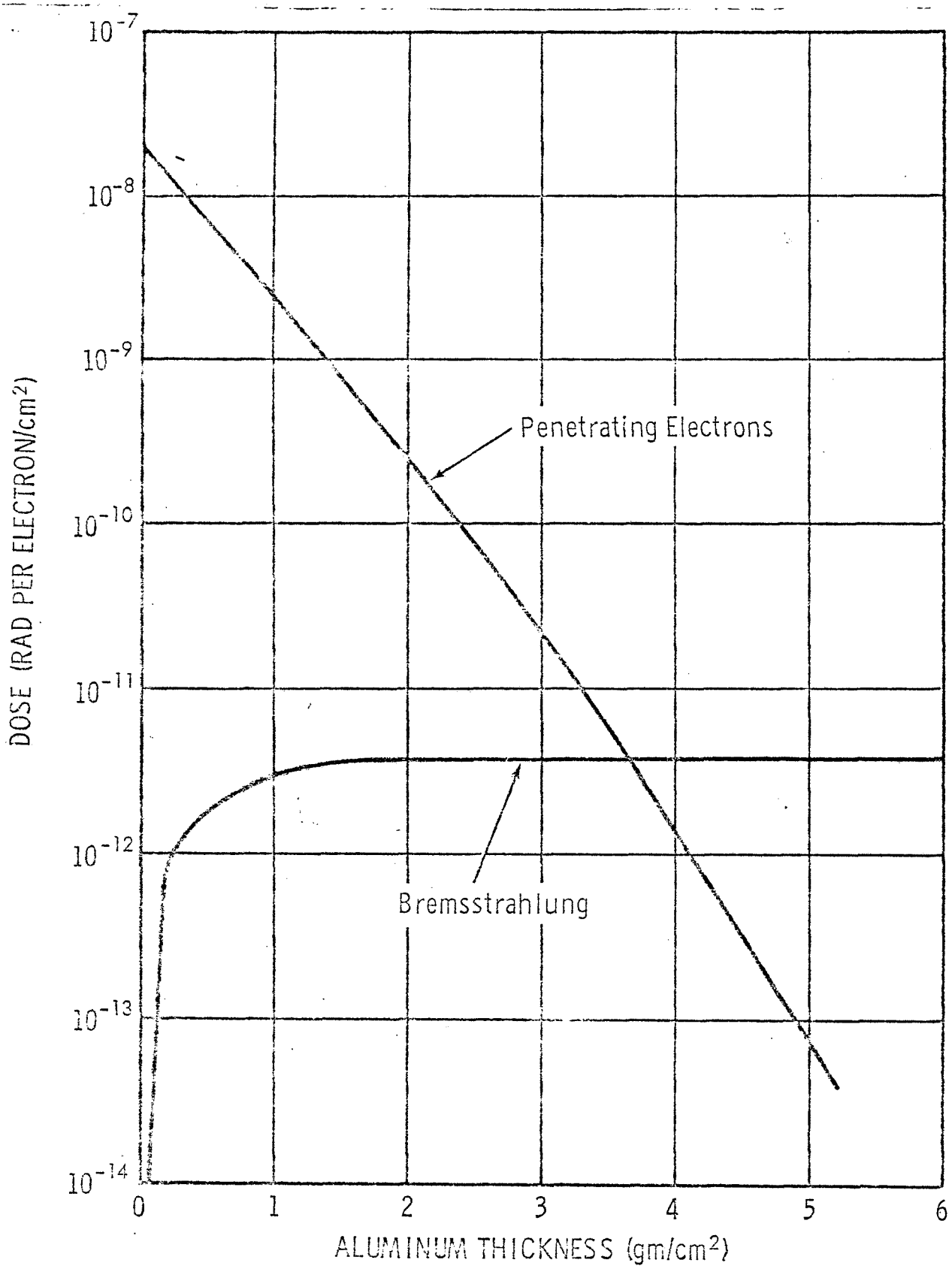

NASA RV63 - 1380

Figure 12. Trapped Radiation Fluxes Encountered in Satellite Orbits

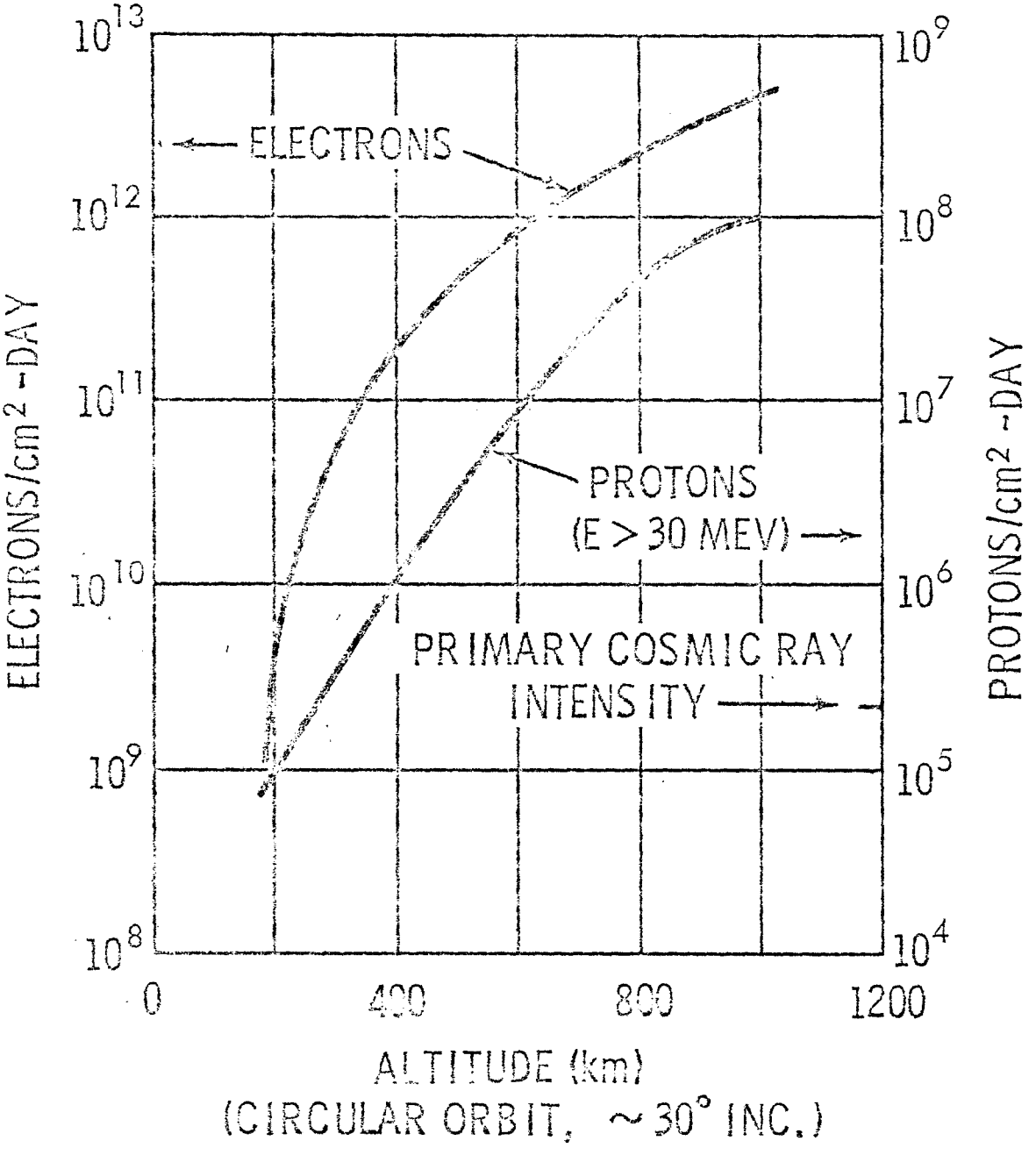

NASA RV63 - 1366

The internal radiation environment depends upon both the penetrating capability of the radiation and the vehicle mission. Most future missions may be categorized, in a broad sense, into groups based on the nature of the radiation environment which will be encountered. In this section several such categories are considered, in a quite general manner, to establish the relative magnitude of the radiation levels from the various sources as a function of shielding thickness. The curves which are presented should be considered only as approximations to the levels and should not be taken as definitive. The artificial electron belt is not included.

Interplanetary Missions - The radiation environment for interplanetary missions will depend to a large extent upon the manner in which the missions are carried out. Consequently, these types of missions are divided into two categories for consideration of the radiation problem. The first category involves those missions which are characterized by high thrust, rapid traversal of the Van Allen radiation belt. The second category, on the other hand, is representative of missions accomplished with low thrust vehicles, such as those utilizing electric propulsion, which spiral slowly through the region of trapped radiation. Curves of radiation intensity as a function of shield thickness for each component are shown for these categories in Figure 13. The intensities are given in rads at the surface of a low Z material.

It is seen that the radiation problems encountered in these two categories differ. In the high thrust case, the problem is primarily

Figure 13. Radiation Environment for Interplanetary Missions

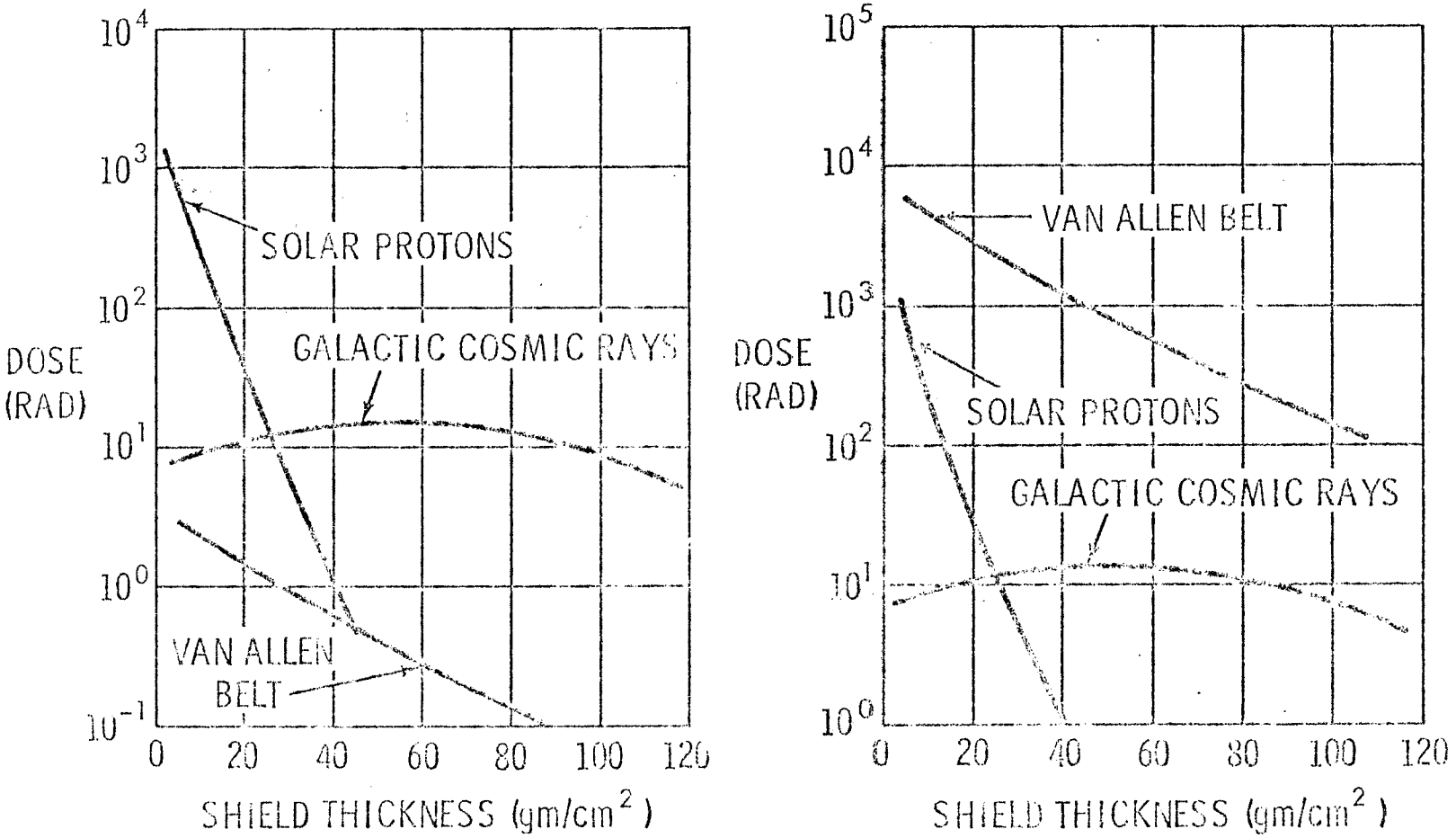

NASA RV63 - 1375

that resulting from solar protons while in the case of the low thrust trajectory the trapped radiation presents the major problem. The difference, of course, arises not through any difference in the solar proton or galactic cosmic ray environments but from the difference in exposure time in the Van Allen belt.

Another source of radiation which may be a factor in interplanetary missions but has not been included in the above considerations is the existence of radiation belts surrounding other planets.

Orbital Missions - The nature of the radiation problem for orbital missions in the region occupied by the natural trapped radiation belt is indicated in Figure 14. Here, the missions may be divided into two general categories (1) those utilizing equatorial orbits and (2) those calling for polar orbits. The curves in Figure 14 are based on a one year period. Contracting or expanding this period would only change the absolute magnitude of the components. The shaded areas indicated for the Van Allen belt radiation are representative of the variation of intensity over altitudes from ~900 to ~7500 Km.

The Van Allen belt is seen to present the major problem for these missions. The chief difference in the radiation environment for the polar orbit as opposed to the equatorial orbit is the disappearance of the solar proton radiation in the latter case. This, of course, is due to the shielding afforded by the earth's magnetic field, as is the variation noted for the galactic cosmic radiation.

Naturally, all orbital operations need not be in the regions between ~900 and ~7500 Km. For orbits at higher altitudes the shielding

Figure 14. Radiation Environment for Vehicles Orbiting in Van Allen Belt

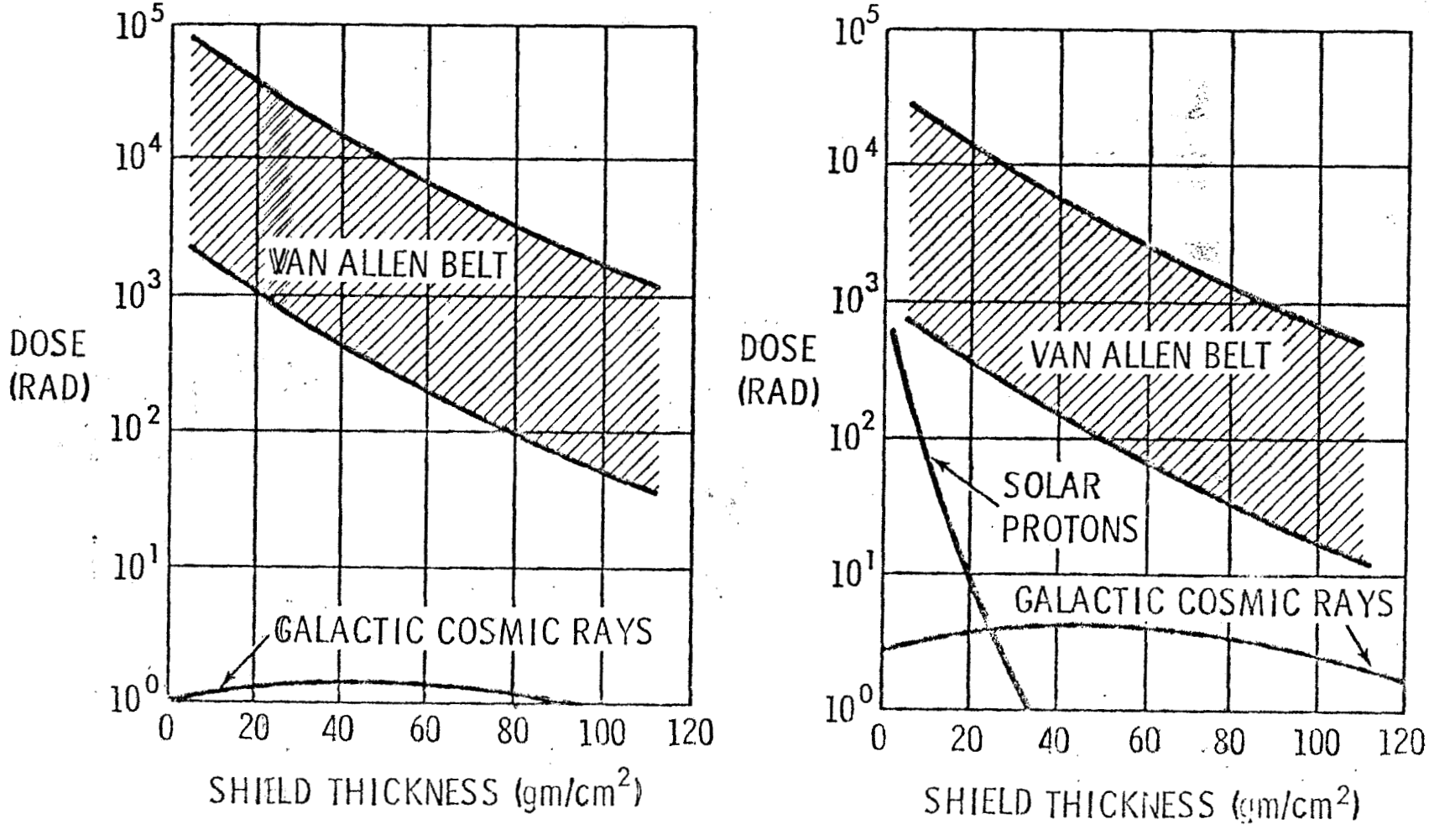

NASA RV63 - 1376

problem slowly approaches the case illustrated in Figure 13(a) while those at lower altitudes approach those shown in Figures 14(a) and 14(b) with the Van Allen component removed.

Conclusions

It is obvious that regardless of its mission any spacecraft will be subjected to a radiation environment. Since the geomagnetically trapped radiation is confined to a relatively small region of space which can be rapidly traversed by high-thrust vehicles, it presents the principal radiation problem only for vehicles orbiting in that region or for low-thrust vehicles spiralling out through the region. However, the radiation environment presented to such vehicles is the most severe that will be encountered as a result of the indigenous radiation.

The solar cosmic radiation which is the dominating radiation environment for deep space vehicles which traverse the trapped radiation belts rapidly is still not completely defined or understood. The short period of time over which these events have been observed does not allow complete confidence in statistical treatment of the problem which must be used or in the maximum possible size of future events. The definition of this environment as well as that of the geomagnetically trapped radiation will doubtlessly undergo several more perturbations before final understanding is achieved.

The galactic cosmic radiation is the most well defined of the natural radiation components but, as would be the case, presents little or no problem from the radiation effects point of view.

The artificial electron belt which resulted from the July 1962 high-altitude nuclear detonation has from the time of formation until now presented a severe radiation environment in an area which previously was practically free of all radiation. Decay of the belt, however, is taking place continually so that its presence will become less and less important.

In general, it can be said that the major radiation effects problems from the indigenous radiations in space will be with items on or near the surface of vehicles. Unfortunately, insufficient data have been gathered on the low energy spectra of the various components to make an accurate assessment of such problems possible at this time.

REFERENCES

1. Malitson, H.H., and Webber, W.R., "A Summary of Solar Cosmic Ray Events", Solar Proton Manual, edited by Frank B. McDonald, Goddard Space Flight Center Report X-611-62-122 (Revised January 25, 1963)

2. Webber, W.R., "Time Variations of Low Energy Cosmic Rays During the Recent Solar Cycle", Progress in Elementary Particle and Cosmic Ray Physics, edited by J.G. Wilson and S.A. Wouthuysen, Amsterdam; North Holland Publ. Co., Vol. 6, 1962

3. Bailey, D.K., "Time Variations of the Energy Spectrum of Solar Cosmic Rays in Relation to the Radiation Hazard in Space", Journal of Geophysical Research, 67, pp. 391-396 (1962)

4. Fichtel, C.E., Guss, D.E., and Ogilvie, K.W., "Details of Individual Solar Particle Events", Solar Proton Manual, edited by Frank B. McDonald, Goddard Space Flight Center Report X-611-62-122 (Revised January 25, 1963)

5. McCracken, Kenneth G., "Anisotropies in Cosmic Radiation of Solar Origin", Solar Proton Manual, edited by Frank B. McDonald, Goddard Space Flight Center Report X-611-62-122 (Revised January 25, 1963)

6. Van Allen, J.A., and Frank, L.A., "Radiation Measurements to 658,300 Kilometers with Pioneer IV", Nature 184, 219-224 (1959)

7. Van Allen, J.A., "Brief Note on the Radiation Belts of the Earth", Proceedings of the Symposium on the Protection Against Radiation Hazards in Space, Gatlinburg, Tennessee, Nov. 5-7, 1962, US AEC TID-7652

8. Allen, R.I., Dessler, A.J., Perkins, J.F., and Price, H.C., "Shield Problems in Manned Space Vehicles", Lockheed Nuclear Products Report No. 104 (1960)

9. McIlwain, Carl E., "Coordinates for Mapping the Distribution of Magnetically Trapped Particles" Journal of Geophysical Research 66 3681-3692 (1961)

10. Freden, S.C., and White, R.S., "Protons in the Earth's Magnetic Field", Physical Review Letters 3, 9-11 (1959)

11. Naugle, J.E., and Kniffen, D.A., "Flux and Energy Spectro of the Protons in the Inner Van Allen Belt", Physical Review Letters, 7, pp 3-6 (1961)

12. McIlwain, C.E., and Pizzella, G., "On the Energy Spectrum of Protons Trapped in the Earth's Inner Van Allen Zone", Journal of Geophysical Research 68, pp 1811-1823 (1963)

13. O'Brien, B.J., Van Allen, J.A., Laughlin, C.D., and Frank, L.A., "Absolute Electron Intensities in the Heart of the Earth's Outer Radiation Zone" Journal of Geophysical Research 67, pp 397-403 (1962)

14. Keller, J.W., Shelton, R.D., Potter, R.A., and Lacy, L., "A Study of the Effect of Geomagnetically Trapped Radiation on Unprotected Solar Cells", Proceeding of the IRE 50, pp 2320-2327 (1962)

15. Hess, W.N., "The Artificial Radiation Belt Made on July 9, 1962" Journal of Geophysical Research 68, pp 667-683 (1963)

16. Carter, R.E., Reines, F., Wagner, J.J., and Wyman, M.E., "Free Antineutrino Absorption Cross Section, 2, Expected Cross Section From Measurements of Fission Fragment Electron Spectrum", Physical Review, 113, 280-286 (1959)

17. Hess, W.N. (private communication)